 DOI: 10.1002/masy.200650105

Kinetics of Temperature-induced and Reaction-induced Phase Separation Studied by Modulated Temperature DSC

*Ronny Pieters, Hans E. Miltner, Guy Van Assche, Bruno Van Mele**

Summary: Temperature-induced phase separation of P(EO75-*ran*-PO25)/PES and reaction-induced phase separation of DGEBA/MDA modified with PVME are studied using MTDSC as an in-situ tool. Phase separation can be probed by the onset of an 'excess' contribution in the MTDSC heat capacity signal, in good correspondence with the cloud point temperature. This feature enables the complete construction of the state diagram of P(EO75-*ran*-PO25)/PES. The detection of phase separation-induced partial vitrification of the high-T_g phase (PES-rich phase) enables to sub-divide the LCST-type heterogeneous region in a *zone 1* (no interference of partial vitrification) and a *zone 2* (interference of partial vitrification of the PES-rich phase). This sub-division of the heterogeneous region has drastic implications on the remixing behavior of demixed blends. In DGEBA/MDA modified with PVME, reaction-induced phase separation accompanied by an increase in reaction rate, followed by a vitrification step of the epoxy-amine phase can be detected in-situ. In non-isothermal conditions, a diffusion-controlled reaction after vitrification and a final devitrification of the system is also observed.

Keywords: blends; curing of polymers; heat capacity; modulated temperature differential scanning calorimetry; phase separation

Introduction

Modulated temperature differential scanning calorimetry (MTDSC) is a powerful extension of conventional DSC, in which a sinusoidal perturbation is superimposed on the underlying temperature program. MTDSC allows for the simultaneous measurement of heat flow, heat capacity and heat flow phase. Kinetic thermal processes in the material, depending on time and absolute temperature, usually appear in the 'non-reversing' heat flow, while properties with heat effects proportional to the heating rate are found in the 'reversing' heat flow (or heat capacity related) signal. This MTDSC deconvolution method turns out to be very valuable for the study of the kinetics in reacting polymer systems [1–6].

This straightforward deconvolution procedure is no longer valid for the characterization of polymer melting/crystallization [7], temperature-induced phase separation (TIPS) in partially miscible polymer blends [8,9], polymer solutions [10–13] and reaction-induced phase separation (RIPS) in reacting polymer systems [14]. Heat effects caused by fast processes, e.g. demixing and remixing, occur during one modulation cycle and thus contribute to the heat capacity signal. This causes an 'excess' contribution in the MTDSC heat capacity signal and gives rise to an 'apparent' heat capacity. The ability to detect small heats of demixing or remixing in the MTDSC heat capacity signal offers interesting perspectives to characterize polymer miscibility and development of morphology in

Polymer Science and Structural Chemistry – POSC, Physical Chemistry and Polymer Science – FYSC, Vrije Universiteit Brussel (VUB), Pleinlaan 2, B-1050 Brussels, Belgium
Fax: +32-(0)2-6293278; Tel: +32-(0)2-6293276 or 3288
E-mail: bvmele@vub.ac.be

polymer blends. The final state and properties of these systems are primarily governed by the kinetics of interfering phase transformations (demixing, remixing, vitrification, crystallization). As the MTDSC heat capacity signal can be measured in (quasi)-isothermal conditions, real-time monitoring of these phase transformations is possible. The observed time-temperature dependencies under controlled conditions provide information on the kinetics and allow to distinguish between fast molecular processes of mixing or demixing (nanoscale miscibility) and long term evolutions (slow processes) on a macroscopic level, such as interphase or morphology development and partial vitrification.

Experimental

Materials

The statistical copolymer containing 75 wt% ethylene oxide and 25 wt% propylene oxide, abbreviated as P(EO75-*ran*-PO25), with a number average molar mass of 2500 $gmol^{-1}$, and poly(ether sulphone) or poly(1,4-phenylene ether sulphone), abbreviated as PES, with a viscosity average molar mass of 20,000 $gmol^{-1}$, were both supplied by Aldrich. A reactive epoxy-amine system was used: a bi-functional epoxy, diglycidyl ether of bisphenol A (DGEBA, Epon 825 from Shell), in combination with appropriate amounts of a tetra-functional amine hardener (methylene dianiline, MDA from Janssen Chimica). A stoichiometric mixture of this pure system was modified with poly(vinyl methylether) with a molar mass of 20,000 $gmol^{-1}$[15] (PVME from Aldrich).

Techniques

Experiments were either performed on a TA Instruments 2920 DSC with the MDSC™ option, equipped with an RCS (Refrigerated Cooling System) cooling accessory and purged with helium (25 $ml.min^{-1}$), or on a TA Instruments Q1000 DSC (Tzero™ DSC-technology) equipped with an RCS cooling accessory and purged with nitrogen (25 $ml.min^{-1}$). Indium was used for temperature calibration of both DSC instruments, in combination with cyclohexane or gallium. Indium was also used for enthalpy calibration. Standard modulation conditions were an amplitude A_T of 0.5 °C and a period p of 60 s. Cloud point temperatures were detected by measuring the (visible) light transmitted through thin samples between glass slides or polymer blend films on glass slides. The slides were mounted in a Mettler Toledo FP82-HT hot stage to impose the desired time-temperature program. The hot stage was placed in a Spectratech optical microscope (magnification ×10).

Results and Discussion

Temperature-Induced Phase Separation

The added value of using the MTDSC heat capacity signal to study temperature-induced phase separation in polymer blends has been demonstrated for the first time for poly(ethylene oxide)/poly(ether sulphone) (PEO/PES) blends, showing LCST-type phase behavior [8,9]. In the present paper, the MTDSC methodology has been extended by replacing PEO in PEO/PES blends with an (ethylene-propylene)oxide copolymer (P(EO75-*ran*-PO25)), also showing LCST-type phase behavior, but where the propylene oxide part reduces miscibility, as evidenced by the decrease of the heterogeneous region to lower temperatures by about 50 °C. Starting from the homogeneous miscible melt, phase separation temperatures can be detected as the onset of an 'excess' heat capacity contribution as a function of temperature (see Figure 1), and this in good correspondence with the 'classical' cloud point temperatures (T_{cl}) determined by optical microscopy (see Figure 2).

All thermal transitions obtained from the MTDSC heat capacity signal for the different blend compositions, i.e., glass transition temperature (T_g), width of glass transition (ΔT_g), end-set temperature of the melting transition (T_m), and phase

separation temperature can be brought together in a state diagram as shown in Figure 2.

Beyond the onset of phase separation, the MTDSC heat capacity signal initially increases, goes through a maximum, and eventually drops below the baseline heat capacity level extrapolated from the homogeneous melt, as shown in Figure 1. This intersection between the MTDSC heat capacity signal and the extrapolated baseline heat capacity occurs at about the same temperature, i.e., around 65 °C, for all the blend compositions, and marks the onset of partial vitrification of the PES-rich coexisting phase. This onset sub-divides the heterogeneous region in a *zone* 1 (no interference with partial vitrification) and a *zone* 2 (interference with partial vitrification of the PES-rich phase). Note that the homogeneous miscible melt region between the end-set temperature of melting and the onset of phase separation is denoted by *zone* 0. The partial vitrification of the PES-rich phase is caused by the intersection of the phase separation curve with the high-temperature end of the glass transition for compositions of high PES-content, while the calculated value of T_g is more than 50 °C lower. This clearly demonstrates the importance of the width of T_g when dealing with polymer blends, as the discrete T_g values are too low and therefore unable to explain the observed phase behavior.

The observation of (partial) vitrification upon heating for non-reactive blends is quite remarkable and – at first sight – surprising, as vitrification in non-reactive blends is only anticipated during cooling. Phase separation-induced partial vitrification, while increasing the temperature, was confirmed by Small Angle Oscillatory Shear Rheometry (not shown).

Temperature-Induced Phase Dissolution

Phase separation-induced partial vitrification has a profound effect on the remixing kinetics. Remixing in *zone* 0 after demixing in *zone* 1 results in fast and almost instantaneous remixing, whereas remixing in *zone* 0 after demixing in *zone* 2 is no longer instantaneous. As a consequence, the remixing kinetics can be monitored in-situ by the recovery of the MTDSC heat capacity signal towards the heat capacity level of the homogeneous melt (devitrification of the PES-rich phase), as shown

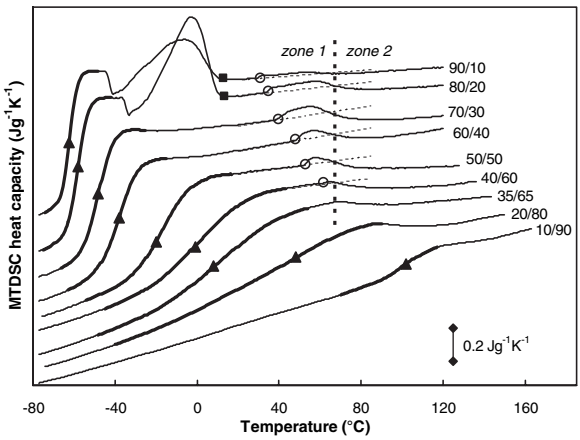

Figure 1.
MTDSC heat capacity for different compositions of P(EO75-*ran*-PO25)/PES 2500/20,000 at a heating rate of 1 °C.min^{-1}: end-set of melting transition T_m (■), MTDSC phase separation temperature (○), homogeneous T_g (▲), width of glass transition ΔT_g (thick full lines); baseline heat capacity extrapolated from the homogeneous melt (thin dashed lines); intersection between apparent heat capacity and baseline heat capacity (thick dashed vertical line); curves have been shifted for clarity.

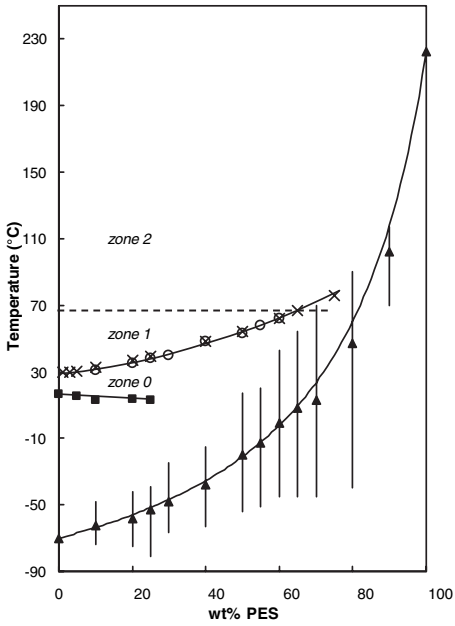

Figure 2.
State diagram for the P(EO75-*ran*-PO25)/PES 2500/20,000 blend obtained by MTDSC at a heating rate of 1 °C.min^{-1}: end-set of melting transition T_m (■), MTDSC phase separation temperature (○), T_{cl} by Optical Microscopy (X), T_g (▲), and ΔT_g (vertical bars); phase separation curve and melting curve represented by thin lines are a guide to the eye; division of the heterogeneous region in *zone* 1 and *zone* 2 by MTDSC (thick dashed lines, see text); Gordon-Taylor T_g-composition relation with $k_{GT} = 0.20$ (thin line).

in Figure 3. Increasing the demixing temperature in *zone* 2 also drastically slows down the remixing behavior in *zone* 0, due to the fact that the PES-rich co-existing phase progresses towards a more vitrified state during demixing. This is mainly caused by the enrichment of the PES-rich co-existing phase with PES at higher demixing temperatures (see Figure 2). Hence, upon cooling the demixed blend to the same remixing temperature in *zone* 0, the PES-rich co-existing phase is in an even more vitrified state compared to the lower demixing temperatures.

Reaction-Induced Phase Separation

Reaction-induced phase separation is a more complicated situation, combining reaction and phase separation induced by the progress of the reaction. The large heat effect of an epoxy-amine cure reaction is found in the non-reversing heat flow and can be linked to the heat evolved when epoxide rings are opened during their reaction with amine functionalities, while the change in the baseline heat capacity induced by the chemical reaction can be found in the MTDSC heat capacity signal [1–6]. As demonstrated in previous paragraphs, the small heat effect accompanying phase separation is expected to arise in the MTDSC heat capacity signal. Indeed, both in quasi-isothermal (see Figure 4) and non-isothermal (see Figure 5) cure conditions of DGEBA/MDA modified with PVME, the onset and heat of the LCST-type phase separation caused by the cure reaction can be found in the MTDSC heat capacity signal, and this onset of the excess contribution in the heat capacity signal nicely corresponds to the 'classical' cloud point (not shown). Moreover, at this onset of phase separation, an increase in reaction rate is also observed in the non-reversing heat flow (see Figure 4 and 5: ●). This acceleration is caused by the higher concentration of the reactive groups in the mobile epoxy-amine phase that was created upon reaction-induced phase separation.

Beyond the onset of reaction-induced phase separation, the heat capacity signal sharply decreases, which is related to the vitrification of the thermoset, i.e., the transition from a liquid or rubbery state to a glassy state due to the progressing reaction and increasingT_g of the system. In non-isothermal conditions, the vitrification step is followed by a diffusion-controlled reaction, seen as a high-temperature tail in the non-reversing heat flow, and at the end by a devitrification step (see Figure 5) [1–6].

The occurrence of reaction-induced phase separation is confirmed by the appearance of two T_g's in the subsequent heating, as opposed to the single T_g observed for the homogeneous mixture prior to reaction (see Figure 5). The reaction might still be going on beyond the devitrification step (the high-temperature

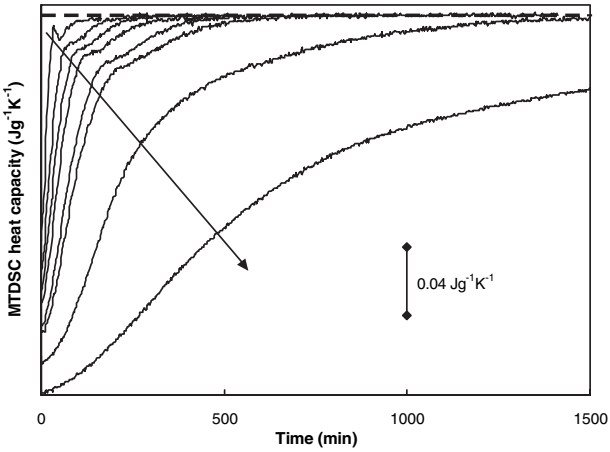

Figure 3.
Quasi-isothermal remixing of P(EO75-*ran*-PO25)/PES 50/50 2500/20,000 at 48.2 °C (*zone* 0) after quasi-isothermal demixing for 15 min in *zone* 2 at increasing demixing temperatures: 77, 79, 81, 83, 85, 87, 96.9, and 106.8 °C (the arrow indicates the increase of the demixing temperature); baseline heat capacity of the homogeneous melt at 48.2 °C indicated by dashed line.

tail of the non-reversing heat flow is still seen beyond the end-set of devitrification), and in combination with a progressing phase separation gives rise to the higher position of the T_g of the full-cured epoxy-amine-rich phase in the second heating of Figure 5 (compare with the end-set of devitrification). The low-temperature phase is almost pure PVME.

Conclusions

The benefits of the MTDSC heat capacity signal for in-situ monitoring of phase separation are nicely illustrated for both temperature-induced and reaction-induced phase separation. Upon temperature-induced phase separation, the fast demixing/remixing processes following the

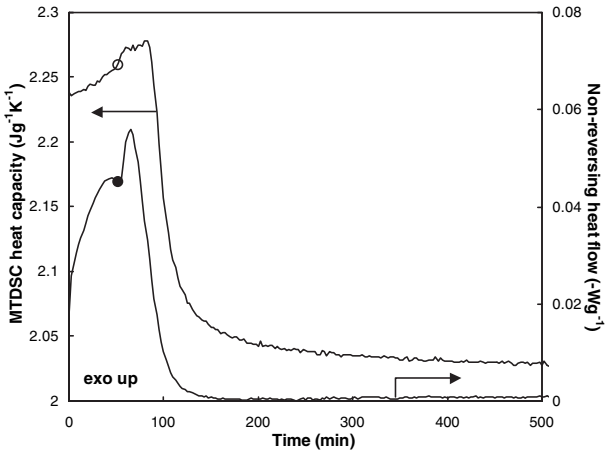

Figure 4.
MTDSC heat capacity and non-reversing heat flow during a quasi-isothermal cure at 100 °C of DGEBA/MDA modified with 30 wt% PVME; MTDSC phase separation temperature by means of the heat capacity signal (○) and the non-reversing heat flow (●).

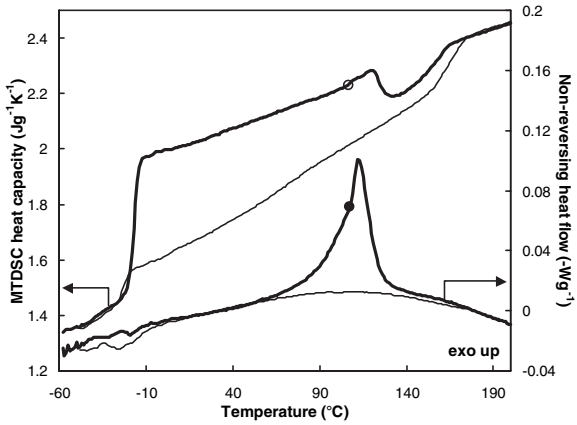

Figure 5.
MTDSC heat capacity and non-reversing heat flow during a non-isothermal cure (thick lines) of DGEBA/MDA modified with 30 wt% PVME and the subsequent heating (thin lines), both at a heating rate of 0.5 °C.min^{-1}; MTDSC phase separation temperature by means of the heat capacity signal (○) and the non-reversing heat flow (●).

applied temperature modulation give rise to an excess contribution, which is superimposed on the baseline heat capacity. This feature enables the complete construction of the state diagram by means of non-isothermal MTDSC heat capacity measurements, including the detection of phase separation-induced partial vitrification of the high-T_g phase. This phase separation-induced vitrification divides the heterogeneous region in a *zone* 1 (no interference with partial vitrification) and a *zone* 2 (interference with partial vitrification of the high-T_g phase). Moreover, this subdivision of the heterogeneous region has drastic implications on the remixing behavior of demixed blends. Upon reaction-induced phase separation, again an excess contribution arises in the MTDSC heat capacity signal, both under non-isothermal and quasi-isothermal conditions, while the higher concentration of the reactive groups in the mobile epoxy-amine phase causes an increase in reaction rate, which is found in the non-reversing heat flow.

[1] G. Van Assche, A. Van Hemelrijck, H. Rahier, B. Van Mele, *Thermochim. Acta* **1995**, *268*, 121.
[2] G. Van Assche, A. Van Hemelrijck, H. Rahier, B. Van Mele, *Thermochim. Acta* **1996**, *286*, 209.
[3] G. Van Assche, A. Van Hemelrijck, H. Rahier, B. Van Mele, *Thermochim. Acta* **1997**, *305*, 317.
[4] S. Swier, G. Van Assche, A. Van Hemelrijck, H. Rahier, E. Verdonck, B. Van Mele, *J. Therm. Anal. Calorim.* **1998**, *54*, 585.
[5] S. Swier, B. Van Mele, *Thermochim. Acta* **1999**, *330*, 175.
[6] S. Swier, B. Van Mele, *Macromolecules* **2003**, *36*, 4424.
[7] H. E. Miltner, H. Rahier, A. Pozsgay, B. Pukánszky, B. Van Mele, *Compos. Interfaces* 2005, in press.
[8] G. Dreezen, G. Groeninckx, S. Swier, B. Van Mele, *Polymer* **2001**, *42*, 1449.
[9] S. Swier, R. Pieters, B. Van Mele, *Polymer* **2002**, *43*, 3611.
[10] P. C. van der Heijden, M. Mulder, M. Wessling, *Thermochim. Acta* **2001**, *378*, 27.
[11] S. Swier, K. Van Durme, B. Van Mele, *J. Polym. Sci., Part B: Polym. Phys.* **2003**, *41*, 1824.
[12] K. Van Durme, S. Verbrugghe, F. E. Du Prez, B. Van Mele, *Macromolecules* **2004**, *37*, 1054.
[13] K. Van Durme, G. Van Assche, B. Van Mele, *Macromolecules* **2004**, *37*, 9596.
[14] S. Swier, B. Van Mele, *Polymer* **2003**, *44*, 2689.
[15] E. Nies, A. Ramzi, H. Berghmans, T. Li, R. K. Heenan, S.M. King, *Macromolecules* **2005**, *38*, 915.

